NJC

PAPER

View Article Online
View Journal

Cite this: DOI: 10.1039/d0nj04138f

Amine-functionalized metal–organic framework-based Pd nanoparticles: highly efficient multifunctional catalysts for base-free aerobic oxidation of different alcohols†

Abu Taher, *[ab] Md. Abu Bin Hasan Susan, [c] Noorjahan Begum[d] and Ik-Mo Lee *[b]

A palladium (Pd) nanoparticle containing a metal organic framework (MOF) is described as a highly efficient multifunctional catalyst for the aerobic oxidation of different aliphatic, aromatic and heteroaromatic alcohols in toluene. The catalytic efficiency was demonstrated by the high conversion of various reactants with 100% selectivity under mild reaction conditions, where a wide range of reactants are selectively converted into their corresponding products in excellent yields (up to 98%). The unique texture of the prepared catalyst was well maintained after several recycling cycles of the catalyst. The catalyst could be reused multiple times without further pre-treatment or any extra precautions for further catalytic cycles. Importantly, the recovery, reusability and excellent selectivity of the prepared catalyst for aerobic oxidation are the remarkable advantages of this method. More importantly, this study has demonstrated the great potential of MOF-based palladium nanoparticles as efficient multifunctional catalysts, while the reaction proceeded smoothly without any external base additives and co-catalysts.

Received 16th August 2020,
Accepted 19th October 2020

DOI: 10.1039/d0nj04138f

rsc.li/njc

Introduction

The oxidation of alcohols to their corresponding aldehydes and ketones is one of the most important reactions in organic synthesis due to the wide-ranging utility of these carbonyl compounds for different purposes in various branches of pure and applied sciences.[1] Modern organic chemistry typically represents a number of methods to affect these alcohol oxidations, and among the most widely featured oxidants are unwanted heavy-metal oxides, such as potassium permanganate, manganese dioxide, pyridinium chlorochromate, pyridinium dichromate, and Jones reagent.[2] These chemical reagents have found widespread applications in pharmaceuticals, agrochemicals, and functional materials, but they are toxic, corrosive, flammable, and difficult to dispose.[2–4] Unfortunately, these reactions result in large quantities of extremely hazardous substances and call for the use of stoichiometric quantities of highly moisture-sensitive, unrecoverable, and expensive chemical reagents that may pose serious health risks.[5] Importantly, satisfactory results were found in only a few cases, in which a large number of expensive additives were required, and this was usually achieved under relatively harsh reaction conditions. Conversely, air is an extremely convenient terminal oxidant due to its abundance, cost effectiveness, ease of use and promising high oxidation potential,[6] which generates no toxic by-products.[7]

On the other hand, metal–organic frameworks (MOFs) are newly developed attractive functional crystalline porous materials,[8] which are successfully applied in versatile branches of pure and applied sciences.[9,10] The most attractive feature of MOFs is their well-ordered porous network structures with a wide range of tunable pore sizes, extremely high surface areas, porosity, and surface functionality.[11] These key features, along with other topological properties, make them suitable candidates for a broad range of uses in catalytic engineering.[12] These catalysts can be easily separated and reused after the reaction,[13] which is highly desirable for cost-effectiveness and green synthesis considerations. In addition, palladium, as a rare earth transition metal, is considered to be one of the most attractive catalysts for use in the oxidation of alcohols[14] due to

---

[a] *Department of Industrial and Production Engineering, European University of Bangladesh, Mirpur, Dhaka-1216, Bangladesh. E-mail: drtaher@eub.edu.bd; Tel: +88-01712-681890*
[b] *Department of Chemistry, Inha University, Incheon 402-751, South Korea. E-mail: imlee@inha.ac.kr; Fax: +82-32-867-5604; Tel: +82-32-860-7682*
[c] *Department of Chemistry, University of Dhaka, Dhaka 100, Bangladesh*
[d] *Department of Agricultural Chemistry, Sher-e-Bangla Agricultural University, Dhaka, Bangladesh*

† Electronic supplementary information (ESI) available: Synthetic details, digital images, EDX spectrum, N_2 adsorption–desorption isotherms, pore volume *vs.* diameter curve, XPS spectra, X-ray powder diffraction, effect of catalyst loading and FTIR spectra. See DOI: 10.1039/d0nj04138f

its nominal features of high catalytic efficiency. In particular, MOF–metal complexes have been demonstrated to exhibit excellent performance for various alcohol oxidations.[15] Until now, even though many excellent MOF–metal catalytic methods have been published,[16] there are only a very limited number of studies on MOF–Pd catalytic methods for aerobic oxidation.[17] In addition, several research groups have reported base-free catalytic oxidation using a hydrogen acceptor (ligand).[18] However, to the best of our knowledge, only a few MOF–metal systems of base-free catalytic oxidation have been described to perform this reaction.[19]

Importantly, aerobic oxidations catalysed by palladium (Pd) have been known for decades, but in spite of the remarkable progress proposed by these oxidations the relatively low catalyst performance due to Pd deactivation still remains challenging in most catalytic reactions.[20] In appropriate ligation environments Pd^0 can be reoxidized by O_2[21] while suppressing the Pd (black) formation in the catalytic cycle by ancillary air-stable ligands such as amines, pyridines and sulfoxides.[22] More importantly, a lot of catalytic systems[15–17] have been developed after decades of research on catalysis, but there are still some drawbacks including low product selectivity[23] that restrict its target product formation; the usage of other materials[24,25] as a cocatalyst makes it economically inefficient and the usage of a base additive[26–28] severely restricts its industrial applications due to corrosion and scale formation. Therefore, a properly designed heterogeneous catalyst with a unique character could not only benefit high catalytic activity and product selectivity but also suppress byproduct formation. Herein, a novel multifunctional MOF–Pd nanoparticle (NP)-based catalytic method was proposed for the aerobic oxidation of various alcohols under cocatalyst free and base free conditions (Scheme 1). In this type of catalytic system, we expected that (i) the amine moiety would show a base effect, (ii) the controlled pore might facilitate catalytic activity and product selectivity, and (iii) the MOF–Pd interaction would show a faster reaction rate due to its synergistic effect (Fig. 1). In this study, we describe the preparation of MOF–Pd NPs (**2B**) and demonstrate their excellent multifunctional activity in the aerobic oxidation of different aliphatic, aromatic and hetero-aromatic alcohols under mild reaction conditions.

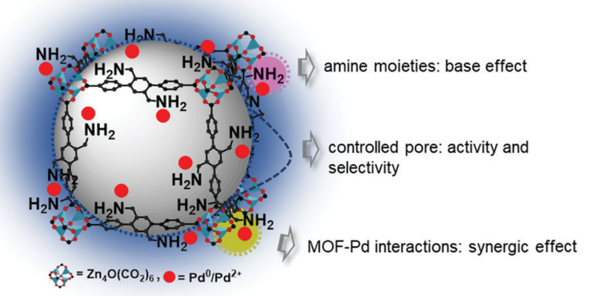

Fig. 1 Concept of amine-functionalized MOF-based Pd nanoparticles (**2B**) as multifunctional catalysts.

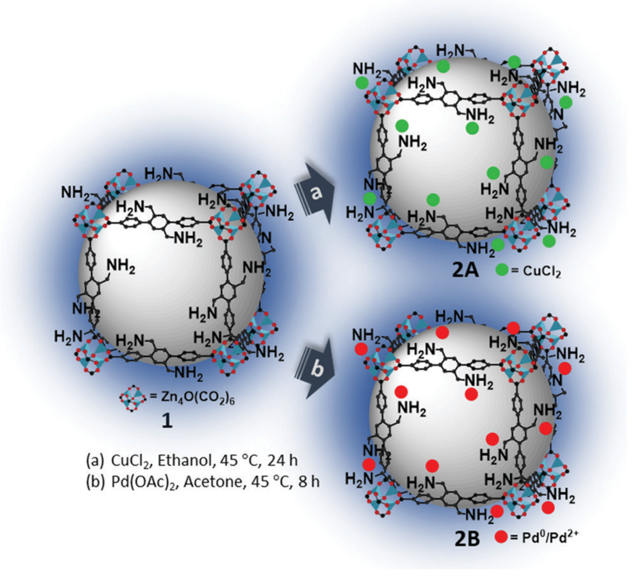

Scheme 1 Post-functionalization route of MOF-based copper nanoparticles (**2A**)[25] and palladium nanoparticles (**2B**).

Results and discussion

An amine-functionalized compound (**1**) was prepared from the azide functional group containing an organic linker ($C_{22}H_{16}N_6O_4$) with $Zn(NO_3)_2 \cdot 6H_2O$ in *N*,*N*-diethylformamide (DEF). Subsequently, we attempted to reduce the azide to amine functional groups using triphenylphosphine (PPh_3) in DEF, as described in our earlier report.[29] The XRD patterns and FTIR spectra of the as-synthesized compound **1** were quite indistinguishable in appearance to those described in the literature[29,30] (Fig. 3a and b, respectively). Furthermore, the elemental analysis of compound **1** was in good agreement with the values calculated from the unit cell dimensions (Table S1, ESI†). Catalyst **2B** was prepared by loading the Pd precursor, palladium(II) acetate, into **1** in acetone. The colour of the solution changed from yellow to completely colourless and the digital microscope observation illustrated that there was no apparent damage to the shape of the crystals after modification (Fig. S1, ESI†). The final products were harvested by simple filtration, washing, and drying to afford **2B** as dark solids (Fig. S1, ESI†). The palladium complexes were anchored on the amine-functionalized MOFs through coordination.[31] The presence of the Pd complexes was confirmed *via* FTIR, XRD, HRSEM, FETEM, XPS, EDS, TGA and ICP analyses. The loading of Pd in **1** was 8.33 wt%, which was detected *via* inductively coupled plasma atomic emission spectroscopy (ICP-AES).

The morphology of catalyst **2B** was observed *via* SEM and TEM analyses. The HRSEM images at different magnifications clearly demonstrated the fine surface morphology in Fig. 2a, b and Fig. S2 (ESI†) and the FETEM images at different magnifications of catalyst **2B** demonstrated homogeneous distribution of Pd NPs on the surface in Fig. 2c and Fig. S2 (ESI†), while

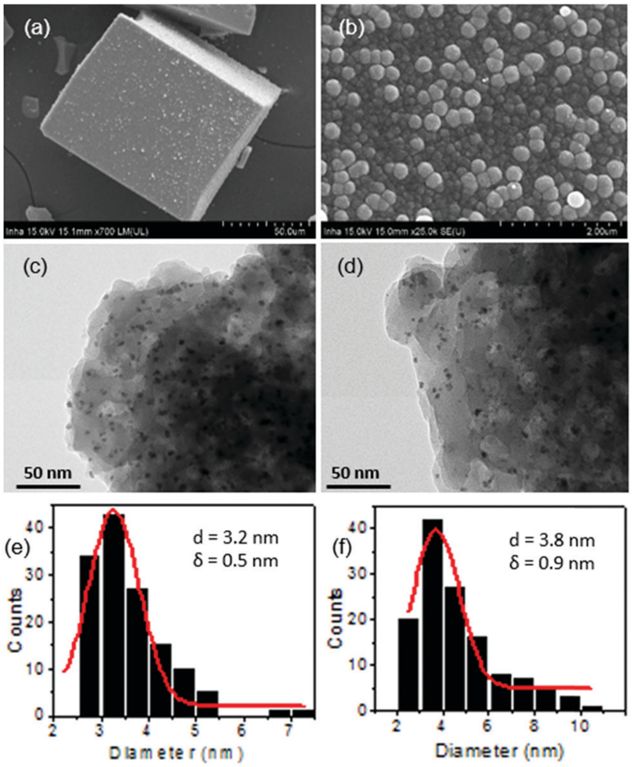

Fig. 2 HRSEM images of the surface of **2B** at different magnifications (scale bars are shown at the bottom) for 50 μm and 2 μm, respectively (a and b); FETEM images of **2B** fresh (c) and after the 5th run (d) in alcohol oxidation; particle size distribution histograms of catalyst **2B** and after the 5th run (e and f), respectively.

the average particle size of Pd nanoparticles (NPs) was 3.2 ± 0.5 nm (Fig. 2e). Furthermore, the SEM image, and corresponding elemental mapping by energy-dispersive X-ray (EDX) spectroscopic analysis (EDS) of **2B**, clearly demonstrated the uniform arrangement of Pd NPs in the amine-functional MOF network (Fig. S3, ESI†). Importantly, the successful loading of Pd in **2B** was confirmed by EDX analysis (Fig. S4, ESI†). A clear Pd peak was resolved when we probed selected area 1 on the Pd loaded MOFs and we also observed a similar EDX spectrum when we probed area 2. It can be noted that the FTIR spectrum of compound **2B** exhibited a new band at 1611 cm^{-1}, which may be attributed to vibration of the acetate anion[32] (Fig. 3b). In particular, the benzylamine related peaks at 3408 cm^{-1} and 3366 cm^{-1} shifted to lower wavenumbers at 3317 cm^{-1} and 3273 cm^{-1}, respectively, in **2B** because of the electron donation from the benzylamine to the Pd center, which resulted in the formation of the MOF–Pd complexes.[25,31] The XRD pattern of the as-prepared **2B** materials demonstrated no apparent changes of the pattern from the starting **1** (Fig. 3a). Significantly, the characteristic XRD peak of Pd (111) at $2\theta = 40^\circ$ is assigned due to the insertion of palladium in **1** as shown in Fig. 3a, which means that the amine-functionalized MOF has coordinated with Pd that is in consonance with earlier reports.[33] In Fig. 3(e), the peak value of Zn $2p_{3/2}$ and Zn $2p_{1/2}$ states that the Zn ions in **2B** were found at 1021.3 eV and 1044.2 eV, respectively, which can be attributed to Zn(II) ions bound to O ions[34] and it is identical to the parent compound. Furthermore, the C–O bands still maintained their positions along with Zn(II) metals, which strongly suggested that the functionalized MOFs were constructed by Zn(II) ions and carboxylate anions with structural similarity (Fig. S5, ESI†). The thermal stability of compound **1** and **2B** was evaluated by thermo-gravimetric analysis (TGA), as depicted in Fig. 3(f). The initial weight loss of both samples at 200 °C can be attributed to loss of water molecules from pores, and the solvent molecules trapped in the MOF structure during synthesis.[35] For catalyst **2B**, a sharp decrease in weight was detected from 260 °C onward, which could be assigned to the loss of loosely bound ligand.[35c] The weight loss of both samples from 260 °C to 450 °C may be due to the decomposition of the organic ligand and the breaking of the MOF network structure.[35c]

N_2 adsorption/desorption isotherm profiles of compounds **1** and **2B** indicate a type I isotherm, which is a characteristic feature of micro-porous materials[36] (Fig. S6, ESI†). Remarkably, the BET surface area and pore volume of **1** were estimated to be 516.19 $m^2\ g^{-1}$ and 0.29 $cm^3\ g^{-1}$, respectively. These results were then compared to precursor **1** where the BET surface area and pore volume of **2B** were reduced to 131.04 $m^2\ g^{-1}$ and 0.06 $cm^3\ g^{-1}$, respectively, which may be attributed to the added mass of palladium species to **1**.[25] In addition, it is observed that after the yellow MOF materials were added into the orange palladium(II) acetate containing acetone solution, the solution turned completely colourless (Fig. S1, ESI†), which once again confirmed the likely formation of the MOF–Pd complexes.

We also performed X-ray photoelectron spectroscopy (XPS) analyses to gain further insights into the oxidation state of Pd in compound **2B**. The asymmetric broadening of Pd (3d) peaks toward higher binding energies suggests that Pd (3d) possesses Pd species in various oxidation states. For quantification, the XPS peaks of Pd ($3d_{5/2,3/2}$) were fitted, resulting in two series of contributing peaks: peaks with binding energies of 335.2 and 340.5 eV were assigned to Pd(0) metal,[37] whereas the peaks at 336.8 and 342.2 eV were assigned to Pd(II)[38] ($3d_{5/2,3/2}$) (Fig. 3c). Comparison of the intensities of the assigned peaks for Pd(0) and Pd(II) in the fitted spectra indicates relative contents of 68% and 32%, respectively. Importantly, the results demonstrated that the Pd species in **2B** are mainly formed as Pd NPs and that the amine groups strongly coordinate with Pd NPs after the reduction.[16b]

The catalytic activity of the as-synthesized catalyst **2B** was examined with a representative set of different aliphatic, aromatic and hetero-aromatic alcohols. Initially, to investigate the catalytic activity of the prepared catalyst **2B**, a series of controlled experiments were carried out under exactly the same reaction conditions (except for **2A**) (Fig. 4). We attempted to conduct the oxidation of benzyl alcohol using air as the oxygen source in the presence of **2B** (1 mol%) under the same reaction conditions (at 80 °C for 3 h) and 100% conversion (GC yield) of benzyl alcohol to benzaldehyde was achieved. We compared these results with those of the same reaction in the presence of (i) **2A**, (ii) **1** + $Pd(OAc)_2$, (iii) $Pd(OAc)_2$, and (iv) **1**. It was found

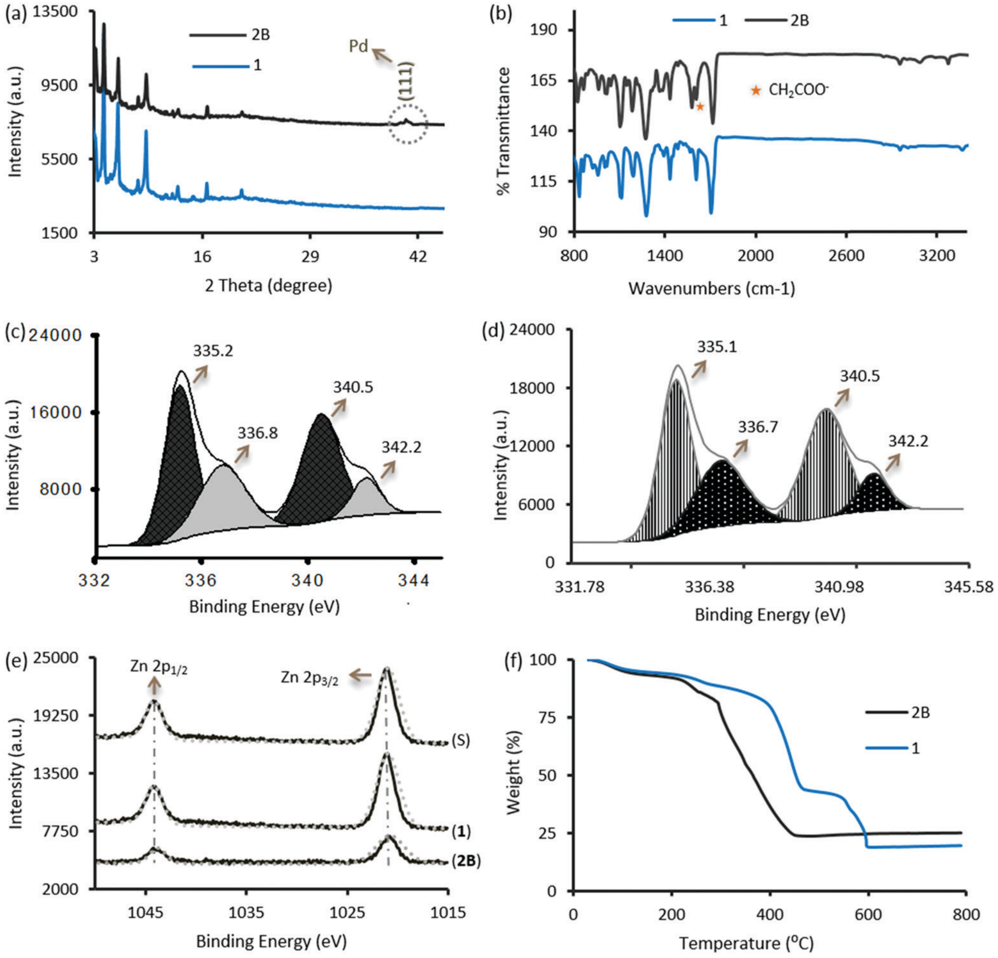

Fig. 3 XRD patterns (a) and FT-IR spectra (b) of compounds **1** and **2B**; XPS spectra of Pd (3d) peaks of catalyst **2B** fresh (c) and after the 5th run (d); high-resolution XPS spectra of Zn 2p peaks of the precursor compound, compound **1**, and catalyst **2B** (e); TGA of compounds **1** and catalyst **2B** (f).

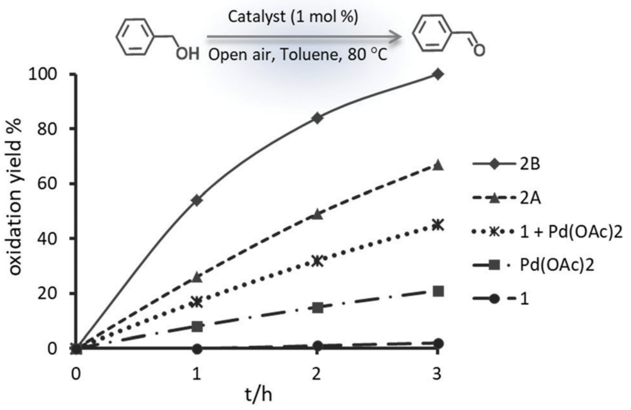

Fig. 4 Aerobic oxidation of benzyl alcohol catalysed by **2B**, **2A**, **1** + $Pd(OAc)_2$, $Pd(OAc)_2$, and **1**; in all the cases the reaction conditions are the same as those listed in Table 1 (entry 1) except **2A** (as reported).[25] The quantity of the product was determined using GC. We calculated an equal amount of Zn^{2+} (when comparing **2A** and **2B** with **1**).

that the oxidation reaction in the presence of **2A** proceeds much faster than the same reaction in the presence of **1** because the Cu(II) species can enhance the reactivity in the presence of the co-catalyst, 2,2,6,6-tetramethyl-piperidyl-1-oxy.[24,25] Interestingly, the use of **2B** allowed the oxidation to proceed significantly faster compared with other catalytic components. This result was consistent with our hypothesis and suggested that the MOF–Pd interactions and controlled pore size of the MOF, enhancing the reactivity as depicted in Fig. 1. In addition, when a mixture of **1** + $Pd(OAc)_2$ or only $Pd(OAc)_2$ was used, relatively poor yields were obtained that may be due to the absence of coordinating ligands.[25,31,39] Importantly, the results demonstrate that the connected ligand between the MOF and the Pd/Cu moieties highly promoted the oxidation of benzyl alcohol to benzaldehyde under base-free conditions. More importantly, catalyst **2B** demonstrated a higher conversion rate on alcohol under the defined conditions without the assistance of a co-catalyst as compared to the earlier reports[24,25] such as catalyst **2A** (Scheme 1). These results suggested that the incorporation of metal Pd into the MOF material could significantly enhance its catalytic activity toward alcohol oxidation.

In order to obtain better catalytic performance, various reaction parameters have been studied to optimize the reaction conditions. In the present study, we examined the effects of the

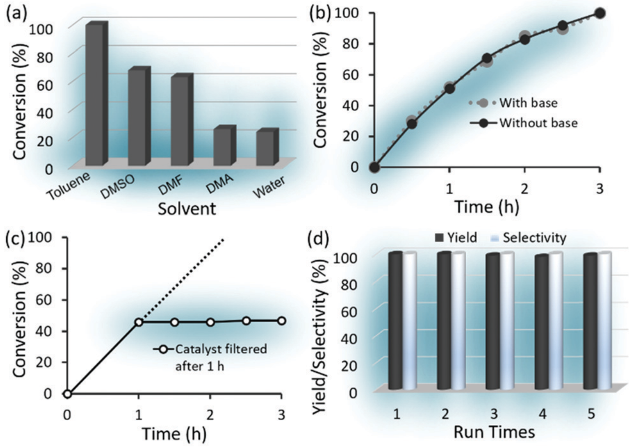

Fig. 5 Aerobic oxidation of benzyl alcohol catalysed by **2B**: (a) reaction in different solvents, (b) effect of the base, (c) hot filtration test, and (d) recyclability of catalyst **2B**. In all cases, the reaction conditions are the same as those listed in Table 1 (entry 1).

Table 1 Aerobic oxidation of various aliphatic, aromatic and hetero-aromatic alcohols catalysed by **2B** in toluene[a]

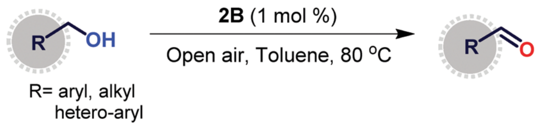

Entry	Substrate	Product	Time (h)	Yield[b] (%)	TON[c]	TOF[d] (h^{-1})
1	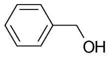	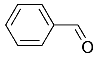	3	98	2642	881
2	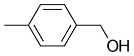	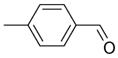	2.3	98	2642	1149
3	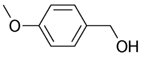	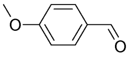	2.5	98	2642	1067
4	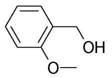	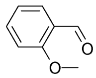	2.7	92	2480	919
5	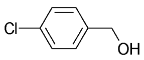	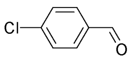	4.5	98	2642	587
6	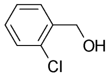	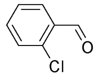	4.7	88	2372	505
7	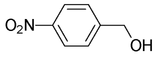	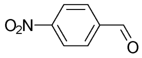	5	98	2642	528
8	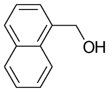	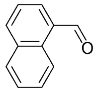	6.5	61	1644	253
9	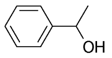	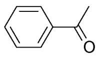	4	98	2642	661
10	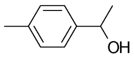	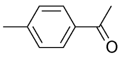	4	96	2588	647
11	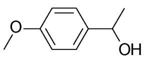	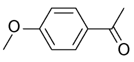	4	96	2588	647
12	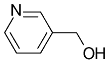	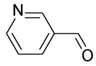	8.5	65	1752	206
13	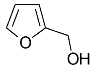	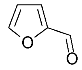	8	64	1725	216
14	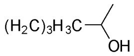	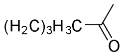	4.5	61	1644	365
15	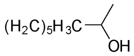	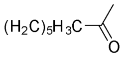	4.5	52	1402	312

[a] Reaction conditions: alcohol (1 mmol), toluene (6 mL) and air as the oxygen source. [b] Isolated yield. Selectivity 100%. [c] TON units (mol product/mol Pd catalyst). [d] TOF units ((mol product/mol Pd cat.) per hour).

solvent and observed that toluene is an excellent solvent for aerobic alcohol oxidation as shown in Fig. 5a. The results revealed the superior catalytic activity of **2B** in toluene medium and it is worth noting that catalyst **2B** demonstrated poor catalytic activity in the water medium. Importantly, the crystal structure of the catalyst deformed when water was used as the solvent due to the highly polar nature of water[40] (Fig. S8, ESI†). We investigated the effect of different bases such as Na_2CO_3 and CsF under the same catalytic conditions, but there were no effects in the presence of bases. In particular, catalyst **2B** catalysed the aerobic oxidation of alcohol in the absence of a base, which was very similar in the presence of K_2CO_3 (Fig. 5b). The MOF–Pd demonstrates a remarkable efficiency for alcohol oxidation without the assistance of a base additive. It was assumed that **2B** plays an important role in oxidation as a catalyst, as well as a base. This is mostly because we believe that the amino group containing the MOF had adequate basicity for deprotonation.[41] Subsequently, we optimised the effect of catalyst loading by varying the amount of catalyst **2B** under similar reaction conditions (Fig. S9, ESI†). The results showed that 1 mol% of Pd displayed the best catalytic performance (98% isolated yield) for alcohol oxidation, suggesting that 1 mol% of **2B** is required for successfully performing the reaction under base-free conditions (Table 1).

To explore the substrate scope of our newly developed catalytic protocol, we performed the **2B**-catalyzed aerobic oxidation using a range of different aliphatic, aromatic and heteroaromatic alcohols under defined conditions. We obtained a high turnover number (TON) and turnover frequency (TOF) of the catalyst and the results are summarized in Table 1. All the reactions proceeded smoothly to give the corresponding aldehydes/ketones with good yields (up to 98%); for instance, for benzyl alcohol the reaction proceeded smoothly to give the corresponding benzaldehyde in high yield (98%) with 100% selectivity (TOF = 881 h^{-1}) under base-free conditions (entry 1), and the product peaks were compared to those reported in the literature.[42] By the attachment of a substituent group to the benzene ring, the electron density and consequently the rates of reactions were either fast or slow depending on the electronic nature or the position of the substituent groups. However, catalyst **2B** was tested with electron-donating group (EDG) containing substrates, such as *p*-tolylmethanol, (4-methoxyphenyl)methanol and (2-methoxyphenyl)methanol, which gave the corresponding aldehydes (entries 2–4) in good yields (92–98%). Subsequently, catalyst **2B** was tested with electron-withdrawing group (EWG) containing substrates such as (4-chlorophenyl)methanol, (2-chlorophenyl)methanol and

(4-nitrophenyl)methanol which also gave the corresponding aldehydes (entries 5–7). Even with the double aromatic ring alcohol, naphthalen-1-ylmethanol, the product was obtained in 61% yield (entry 8) which was substantially lower than those of the other primary alcohols. This could be caused by molecular size and steric hindrance effects. Importantly, the reactivity of the substituted benzene could be strongly influenced by the presence of the EDG on the aromatic ring as reported in the literature.[25] It is noteworthy that the aerobic oxidation of secondary alcohols such as 1-phenylethanol, 1-*p*-tolylethanol and 1-(4-methoxyphenyl)ethanol also gave the corresponding products (entries 9–11) in good yields (96–98%). Unfortunately, with this catalytic system secondary alcohols were a little bit difficult to oxidize probably due to steric interactions.[43] Furthermore, heterocyclic alcohols such as (pyridin-3-yl) methanol and (furan-2-yl)methanol were oxidized to give the corresponding products with moderate yields, while this study showed that reaction times were getting longer for heterocyclic alcohols (entries 12 and 13). In the case of aliphatic alcohols such as hexan-2-ol and octan-2-ol (entries 14 and 15) that also gave the corresponding product, the rate of reaction was lower than those of the benzylic alcohols that may be due to steric hindrance.[44] It is clearly shown that these aerobic heterogeneous conditions are highly efficient for the oxidation of different aliphatic, aromatic and hetero-aromatic alcohols to the corresponding aldehydes or ketones with high yields, with TOFs up to 1149 h^{-1} being reached.

Recently, the use of MOFs as heterogeneous catalysts has received much attention in different areas of organic synthesis, while heterogeneity is thus a critical and important issue for catalysis. However, to assess whether our catalyst **2B** is indeed heterogeneous in nature, we carried out a leaching test by performing the oxidation of benzyl alcohol under optimized reaction conditions, in which the catalyst was removed after 1 h, and the reaction proceeded. As indicated in Fig. 5c, no further reaction took place without **2B** after the initiation of the reaction for oxidation at 3 h, while the possible leaching of Pd after the completion of the reaction was monitored by ICP analysis. This finding indicates that no leaching of the catalytically active sites occurs and that **2B** exhibits a typical heterogeneous catalyst nature, which is attributed to an excellent coordination interaction between Pd metal and the amine functionalized-MOF.[25,31] As a heterogeneous catalyst, **2B** can be repeatedly recycled and reused under optimized conditions. This new catalyst can be easily recovered after each reaction cycle using a simple filtration technique and then recycled for further reactions. We thus carefully carried out the recycling reactions and observed a very similar yield (98–100%) on five consecutive runs with 100% selectivity (Fig. 5d). The conversion and especially the selectivity for the desired product were very similar after 3 h. The TON and TOF at 3 h for benzaldehyde formation from benzyl alcohol were 2642 and 881 h^{-1}, respectively, under the optimized conditions.

The results indicate that the as-prepared catalyst **2B** is highly active and stable against the migration of the active species and suppresses the sintering of Pd NPs. We characterized the reused catalysts after five consecutive runs; the TEM and SEM images of the used catalysts only showed slight aggregation of Pd (Fig. 2d and Fig. S2, ESI†) and the average particle size of Pd NPs was 3.8 ± 0.9 nm (Fig. 2f), which does not affect the activity of the catalyst. Moreover, the XPS and FTIR spectra, and XRD patterns of the catalyst, **2B**, exactly resembled those of the fresh catalyst after reusing several times (Fig. 3d and Fig. S5, S10, respectively, ESI†), suggesting that the structural features of **2B** were retained.

The structurally well-defined pores of MOFs may offer unique advantages for catalytic applications compared with others and thus can make processes more feasible, cost-effective and environmentally friendly.[45] However, the increase of the size of aromatic rings reduces the yields of the corresponding products (Fig. 6). Particularly, for the substrate benzyl alcohol, the size of which (4.9 Å) is smaller than the pore size of **2B** (Fig. S6 and S7, ESI†), the yield was up to 98% after 3 h. On the other hand, by increasing the number of aromatic rings or size (8.1 Å), naphthalen-1-ylmethanol gave a much lower yield under the same reaction conditions, suggesting a certain size and shape selectivity. Therefore, this high catalytic activity with excellent selectivity would be due to the large surface area, tunable pore size, and surface functionality, along with other topological properties of the MOF materials.

Experimental

Catalyst preparation

Compounds **1** and **2A** were prepared according to our previously reported procedures.[25] Typically, 1.60 g (6.0 mmol) of triphenylphosphine was dissolved in *N*,*N*-diethylformamide (30 mL) and 0.62 g (0.40 mmol) of the azide functional group containing the MOF was added to the solution in a 50 mL vial. The reaction was carried out without stirring at 80 °C for 10 h in an oil bath. After the starting material had disappeared, compound **1** was found as a light-yellow solid (Fig. S1, ESI†). Then, 0.08 g (0.60 mmol) of copper(II) chloride was dissolved in ethanol (24 mL), and 0.60 g of compound **1** was added to the copper solution. The vial, placed in the oil bath, was heated to

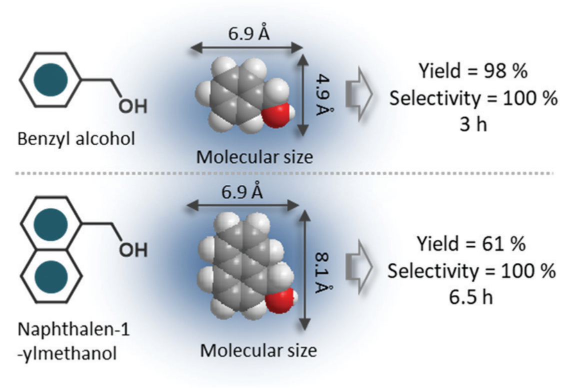

Fig. 6 Size and shape selectivity in the aerobic oxidation of benzyl alcohols and naphthalen-1-ylmethanol using **2B**. In all cases, the reaction conditions are the same as those listed in Table 1.

45 °C for one day, and compound **2A** was given as a blue solid. Similarly, 0.28 g (1.26 mmol) of palladium(II) acetate was dissolved in acetone (20 mL) and 0.60 g (0.42 mmol) of compound **1** was added to the solution. The reaction mixture was placed in the oil bath and heated to 45 °C for 8 h without stirring and the colour of the solution changed from orange to colourless (Fig. S1, ESI†). The crystals were filtered off and washed with fresh acetone (15 mL × 4), and the MOF-based catalyst **2B** was obtained as a dark solid (Fig. S1, ESI†). The catalyst was dried under vacuum and ICP analysis detected 8.33% (wt) Pd in the resulting compound, **2B**.

General procedure for an oxidation reaction

The oxidation of alcohols was carried out in a very simple and easy way such as in a base free, open air system at atmospheric pressure. Typically, to a solution of the substrate (1.00 mmol) in toluene (6 mL) was added **2B** (1 mol%) and the resulting mixture was heated at 80 °C without any base additive under atmospheric air (in an open vial system). The reaction time was determined by checking TLC and GC (Agilent Technologies 7890A GC System). After completion of the reaction, the catalyst was easily filtered off and the filtrate was evaporated under reduced pressure. The separated catalyst was successively reused and recycled for the next reaction without further processing. The crude products were purified *via* column chromatography on silica gel (ethyl acetate–hexane) to give the corresponding product (Table 1) and all the desired products were characterized *via* the comparison of their spectra with those reported in the literature.[42] A hot filtration experiment was carried out according to our previous procedure.[25] Typically, catalyst **2B** was carefully removed from the reaction mixture after 30 minutes of reaction, and the resulting filtrate was heated at 80 °C for an additional 3 h.

Conclusions

In summary, we have designed and developed a novel, highly efficient Pd containing MOF-based multifunctional catalytic system for the aerobic oxidation of various alcohols. In this catalytic system, the catalyst significantly enhanced the reactivity *via* the synergic effect of the MOF–palladium interaction with the controlled pore sizes of MOFs, which increased the reactivity of reactants and maintained 100% selectivity of the products. Importantly, this catalytic method exhibited exclusive practical features that facilitate the oxidation such as without any co-catalysts, faster reaction rates and mild reaction conditions. The results indicate that palladium nanoparticles play a central role in the catalytic reaction without the assistance of any base additives. We believe that this catalytic method will inspire our concurrent inquiry into the applications of these catalytic matrices in the fields of organic synthesis and catalytic engineering.

Conflicts of interest

There are no conflicts to declare.

Acknowledgements

This work was supported by an Inha University Research Grant (Inha 2017).

Notes and references

1 (*a*) R. A. Sheldon and J. K. Kochi, *Metal-Catalyzed Oxidation of Organic Compounds*, Academic Press, New York, 1981; (*b*) M. Hudlicky, *Oxidations in Organic Chemistry*, American Chemical Society, Washington, D.C., 1990; (*c*) R. A. Sheldon, I. W. C. E. Arends, G. J. Brink and A. Dijksman, *Acc. Chem. Res.*, 2002, **35**, 774–781; (*d*) J. Muzart, *Tetrahedron*, 2003, **59**, 5789–5816; (*e*) M. Baumann and I. R. Baxendale, *Beilstein J. Org. Chem.*, 2013, **9**, 2265–2319.

2 (*a*) I. A. S. Shibley Jr., K. E. Amaral, D. J. Aurentz and R. J. McCaully, *J. Chem. Educ.*, 2010, **87**, 1351–1354; (*b*) I. W. C. E. Arends and R. A. Sheldon, in *Modern Oxidation Methods*, ed. J.-E. Backvall, Wiley VCH, Weinheim, Germany, 2nd edn, 2010, pp. 147–185.

3 B. A. Steinhoff, S. R. Fix and S. S. Stahl, *J. Am. Chem. Soc.*, 2002, **124**, 766–767.

4 (*a*) R. D. Richardson and T. Wirth, *Angew. Chem., Int. Ed.*, 2006, **45**, 4402–4404; (*b*) M. Uyanik and K. Ishihara, *Chem. Commun.*, 2009, 2086–2099; (*c*) M. Uyanik, M. Akakura and K. Ishihara, *J. Am. Chem. Soc.*, 2009, **131**, 251–262.

5 (*a*) P. K. Rai, S. S. Lee, M. Zhang, Y. F. Tsang and K.-H. Kim, *Environ. Int.*, 2019, **125**, 365–385; (*b*) Z. Li, Z. Li, Y. Huang, Y. Jiang, Y. Liu, W. Wen, H. Li, J. Shao, C. Wang and X. Zhu, *ACS Omega*, 2020, **5**, 9724–9732.

6 (*a*) C. Parmeggiani and F. Cardona, *Green Chem.*, 2012, **14**, 547–564; (*b*) M. J. Schultz and M. S. Sigman, *Tetrahedron*, 2006, **62**, 8227–8241; (*c*) J. Muzart, *Tetrahedron*, 2003, **59**, 5789–5816.

7 J.-E. Bäckvall, *Modern Oxidation Methods*, Wiley-VCH, Weinheim, 2nd edn, 2011.

8 (*a*) J. R. Long and O. M. Yaghi, *Chem. Soc. Rev.*, 2009, **38**, 1213–1214; (*b*) J. Jiang, Y. Zhao and O. M. Yaghi, *J. Am. Chem. Soc.*, 2016, **138**, 3255–3265.

9 (*a*) S. Keskin and S. Kızılel, *Ind. Eng. Chem. Res.*, 2011, **50**, 1799–1812; (*b*) R. Ricco, C. Pfeiffer, K. Sumida, C. J. Sumby, P. Falcaro, S. Furukawa, N. R. Champness and C. J. Doonan, *CrystEngComm*, 2016, **18**, 6532–6542; (*c*) Y. Cui, J. Zhang, H. He and G. Qian, *Chem. Soc. Rev.*, 2018, **47**, 5740–5785; (*d*) C. Altintas, G. Avci, H. Daglar, A. N. V. Azar, I. Erucar, S. Velioglu and S. Keskin, *J. Mater. Chem. A*, 2019, **7**, 9593–9608; (*e*) M. Ding, R. W. Flaig, H.-L. Jiang and O. M. Yaghi, *Chem. Soc. Rev.*, 2019, **48**, 2783–2828; (*f*) Y. Xue, S. Zheng, H. Xue and H. Pang, *J. Mater. Chem. A*, 2019, **7**, 7301–7327.

10 (*a*) A. H. Chughtai, N. Ahmad, H. A. Younus, A. Laypkovc and F. Verpoort, *Chem. Soc. Rev.*, 2015, **44**, 6804–6849; (*b*) L. Li, J. He, Y. Wang, X. Lv, X. Gu, P. Dai, D. Liu and X. Zhao, *J. Mater. Chem. A*, 2019, **7**, 1964–1988; (*c*) J. Della Rocca, D. Liu and W. Lin, *Acc. Chem. Res.*, 2011, **44**, 957–968; (*d*) Z. Hu, B. J. Deibert and J. Li, *Chem. Soc. Rev.*, 2014, **43**,

5815–5840; (*e*) H. Li, K. Wang, Y. Sun, C. T. Lollar, J. Li and H. C. Zhou, *Mater. Today*, 2018, **21**, 108–121; (*f*) Z. R. Herm, E. D. Bloch and J. R. Long, *Chem. Mater.*, 2014, **26**, 323–338.

11 (*a*) H. C. Zhou, J. R. Long and O. M. Yaghi, *Chem. Rev.*, 2012, **112**, 673–674; (*b*) H. Furukawa, K. E. Cordova, M. ÓKeeffe and O. M. Yaghi, *Science*, 2013, **341**, 1230444.

12 (*a*) D. Farrusseng, S. Aguado and C. Pinel, *Angew. Chem., Int. Ed.*, 2009, **48**, 7502–7513; (*b*) A. Corma, H. Garcia and F. X. Llabres i Xamena, *Chem. Rev.*, 2010, **110**, 4606–4655; (*c*) M. Yoon, R. Srirambalaji and K. Kim, *Chem. Rev.*, 2012, **112**, 1196–1231; (*d*) J. Gascon, A. Corma, F. Kapteijn and F. X. Llabres i Xamena, *ACS Catal.*, 2014, **4**, 361–378; (*e*) J. W. Liu, L. F. Chen, H. Cui, J. Y. Zhang, L. Zhang and C. Y. Su, *Chem. Soc. Rev.*, 2014, **43**, 6011–6061.

13 (*a*) X. Feng, C. Xu, Z.-Q. Wang, S.-F. Tang, W.-J. Fu, B.-M. Ji and L.-Y. Wang, *Inorg. Chem.*, 2015, **54**, 2088–2090; (*b*) Y. Qi, Y. Luan, J. Yu, X. Peng and G. Wang, *Chem. – Eur. J.*, 2015, **21**, 1589–1597; (*c*) J. Wang, F.-W. Ding, J.-P. Ma, Q.-K. Liu, J.-Y. Cheng and Y.-B. Dong, *Inorg. Chem.*, 2015, **54**, 10865–10872.

14 W. C. Ho, K. Chung, A. J. Ingram and R. M. Waymouth, *J. Am. Chem. Soc.*, 2018, **140**, 748–757.

15 (*a*) M. Y. Masoomi, A. Morsali, A. Dhakshinamoorthy and H. Garcia, *Angew. Chem., Int. Ed.*, 2019, **58**, 15188–15205; (*b*) J.-C. Wang, F.-W. Ding, J.-P. Ma, Q.-K. Liu, J.-Y. Cheng and Y.-B. Dong, *Inorg. Chem.*, 2015, **54**, 10865–10872; (*c*) X. Feng, C. Xu, Z.-Q. Wang, S.-F. Tang, W.-J. Fu, B.-M. Ji and L.-Y. Wang, *Inorg. Chem.*, 2015, **54**, 2088–2090; (*d*) X. Zhang, W. Dong, Y. Luan, M. Yang, L. Tan, Y. Guo and H. Gao, *J. Mater. Chem. A*, 2015, **3**, 4266–4273.

16 (*a*) G. Chen, S. Wu, H. Liu, H. Jiang and Y. Li, *Green Chem.*, 2013, **15**, 230–235; (*b*) X. Li, Z. Guo, C. Xiao, T. W. Goh, D. Tesfagaber and W. Huang, *ACS Catal.*, 2014, **4**, 3490–3497.

17 (*a*) M. Zhao, K. Deng, L. He, Y. Liu, G. Li, H. Zhao and Z. Tang, *J. Am. Chem. Soc.*, 2014, **136**, 1738–1741; (*b*) G. Chen, S. Wu, H. Liu, H. Jiang and Y. Li, *Green Chem.*, 2013, **15**, 230–235; (*c*) X. Li, Z. Guo, C. Xiao, T. W. Goh, D. Tesfagaber and W. Huang, *ACS Catal.*, 2014, **4**, 3490–3497.

18 (*a*) S. Murahashi, T. Naota, K. Ito, Y. Maeda and H. Taki, *J. Org. Chem.*, 1987, **52**, 4319–4327; (*b*) Y. Lin, X. Zhu and Y. Zhou, *J. Organomet. Chem.*, 1992, **429**, 269–274; (*c*) Y. Endo and J.-E. Baeckvall, *Chem. – Eur. J*, 2011, **17**, 12596–12601; (*d*) T. Buntara, S. Noel, P. H. Phua, I. Melian-Cabrera, J. G. de Vries and H. Heeres, *Angew. Chem., Int. Ed.*, 2011, **50**, 7083–7087; (*e*) S. Mannam, S. Alamsetti, S. K. Alamsetti and G. Sekar, *Adv. Synth. Catal.*, 2007, **349**, 2253–2258; (*f*) Q. Wang, Y. Zhang, G. Zheng, Z. Tian and G. Yang, *Catal. Commun.*, 2011, **14**, 92–95.

19 W. Zhong, H. Liu, C. Bai, S. Liao and Y. Li, *ACS Catal.*, 2015, **5**, 1850–1856.

20 (*a*) A. N. Campbell and S. S. Stahl, *Acc. Chem. Res.*, 2012, **45**, 851–863; (*b*) L. Jin and A. Lei, *Sci. China: Chem.*, 2012, **55**, 2027–2035; (*c*) Z. Shi, C. Zhang, C. Tang and N. Jiao, *Chem. Soc. Rev.*, 2012, **41**, 3381–3430.

21 (*a*) K. M. Gligorich and M. S. Sigman, *Chem. Commun.*, 2009, 3854–3867; (*b*) S. S. Stahl, *Science*, 2005, **309**(5742), 1824–1826; (*c*) N. N. H. M. Eisink, A. J. Minnaard and M. D. Witte, *Synthesis*, 2017, 822–829.

22 D. Wang, A. B. Weinstein, P. B. White and S. S. Stahl, *Chem. Rev.*, 2018, **118**, 2636–2679.

23 (*a*) S. Wasmus, E. Cattaneo and W. Vielstich, *Electrochim. Acta*, 1990, **35**, 771–775; (*b*) B. Jermann and J. Augustynski, *Electrochim. Acta*, 1994, **39**, 1891–1896; (*c*) J. Xie, Y. Huang and H. Yu, *Front. Environ. Sci. Eng.*, 2015, **9**, 861–866.

24 (*a*) A. Dhakshinamoorthy, M. Alvaro and H. Garcia, *ACS Catal.*, 2011, **1**, 48–53; (*b*) M. Paul, N. N. Adarsh and P. Dastidar, *Cryst. Growth Des.*, 2014, **14**, 1331–1337; (*c*) L. C. Li, R. Matsuda, I. Tanaka, H. Sato, P. Kanoo, H. J. Jeon, M. L. Foo, A. Wakamiya, Y. Murata and S. Kitagawa, *J. Am. Chem. Soc.*, 2014, **136**, 7543–7546.

25 A. Taher, D. W. Kim and I.-M. Lee, *RSC Adv.*, 2017, **7**, 17806–17812.

26 (*a*) R. Noyori and T. Ohkuma, *Angew. Chem., Int. Ed.*, 2001, **40**, 40–73; (*b*) X. Wu and J. Xiao, *Chem. Commun.*, 2007, 2449–2466.

27 (*a*) S. Doherty, J. G. Knight, A. L. Bell, R. W. Harringtonand and W. Clegg, *Organometallics*, 2007, **26**, 2465–2468; (*b*) T. Leyssens, D. Peeters and J. N. Harvey, *Organometallics*, 2008, **27**, 1514–1523.

28 V. Rautenstrauch, X. Hoang-Cong, R. Churlaud, K. Abdur-Rashid and R. H. Morris, *Chem. – Eur. J.*, 2003, **9**, 4954–4967.

29 A. Taher, D.-J. Lee, B.-K. Lee and I.-M. Lee, *Synlett*, 2016, 1433–1437.

30 Y. Goto, H. Sato, S. Shinkai and K. Sada, *J. Am. Chem. Soc.*, 2008, **130**, 14354–14355.

31 A. Taher, D.-J. Lee and I.-M. Lee, *Synlett*, 2016, 2333–2338.

32 N. P. Pawlowicz, R. V. Grondelle, I. H. M. V. Stokkum, J. Breton, M. R. Jones and M. L. Groot, *Biophys. J.*, 2008, **95**, 1268–1284.

33 S. Gao, N. Zhao, M. Shu and S. Che, *Appl. Catal., A*, 2010, **388**, 196–201.

34 M. Shatnawi, A. M. Alsmadi, I. Bsoul, B. Salameh, M. Mathai, G. Alnawashi, G. M. Alzoubi, F. A. Dweri and M. S. Bawa'aneh, *Results Phys.*, 2016, **6**, 1064–1071.

35 (*a*) Z. Ghiamaty, A. Ghaffarinejad, M. Faryadras, A. Abdolmaleki and H. Kazemi, *J. Nanostruct. Chem.*, 2016, **6**, 299–308; (*b*) W. Sun, X. Li, C. Sun, Z. Huang, H. Xu and W. Shen, *Catalysts*, 2019, **9**, 682; (*c*) H. Alamgholiloo, S. Rostamnia, A. Hassankhani, J. Khalafy, M. M. Baradarani, G. Mahmoudi and X. Liu, *Appl. Organomet. Chem.*, 2018, e4539.

36 (*a*) K. A. Cychosz and M. Thommes, *Engineering*, 2018, **4**, 559–566; (*b*) F. J. Sotomayor, K. A. Cychosz and M. Thommes, *Acc. Mater. Surf. Res.*, 2018, **3**, 34–50.

37 R. J. Kalbasi and N. Mosaddegh, *Mater. Res. Bull.*, 2012, **47**, 160–166.

38 G. Zheng, K. Kaefer, S. Mourdikoudis, L. Polavarapu, B. Vaz, S. E. Cartmell, A. Bouleghlimat, N. J. Buurma and L. Yate, *J. Phys. Chem. Lett.*, 2015, **6**, 230–238.

39 C. Bai, Q. Zhao, Y. Li, G. Zhang, F. Zhang and X. Fan, *Catal. Lett.*, 2014, **144**, 1617–1623.

40 A. Dhakshinamoorthy, A. M. Asiri and H. Garcia, *Chem. Commun.*, 2014, **50**, 12800–12814.

41 S. Mannam, S. K. Alamsetti and G. Sekar, *Adv. Synth. Catal.*, 2007, **349**, 2253–2258.

42 (*a*) G. Zhang, X. Han, Y. Luan, Y. Wang, X. Wen and C. Ding, *Chem. Commun.*, 2013, **49**, 7908–7910; (*b*) C. Bai, A. Li, X. Yao, H. Liu and Y. Li, *Green Chem.*, 2016, **18**, 1061–1069.

43 (*a*) R. H. Liu, X. M. Liang, C. Y. Dong and X. Q. Hu, *J. Am. Chem. Soc.*, 2004, **126**, 4112–4113; (*b*) J. L. Long, X. Q. Xie, J. Xu, Q. Gu, L. M. Chen and X. X. Wang, *ACS Catal.*, 2012, **2**, 622–631.

44 M. E. Assal, M. Kuniyil, M. Khan, A. Al-Warthan, M. R. H. Siddiqui, W. Tremel, M. N. Tahir and S. F. Adil, *ChemistryOpen*, 2017, **6**, 112–120.

45 S. L. James, *Chem. Soc. Rev.*, 2003, **32**, 276–288.